Medical diagnosis by using the motion information in image sequences

Cristian Grava*, Bertrand Augereau**, Adriana Grava*

*Faculty of Electrical Engineering and Information Technology,
University of Oradea,
410087 Oradea, Romania, E-Mail: cgrava@uoradea.ro

**Department of Signal, Image and Communications,
University of Poitiers,
86962 Poitiers, France, E-Mail: augereau@sic.sp2mi.univ-poitiers.fr

Abstract ***– This paper consist in a comparative study between some differential motion estimation methods that could be applied in the case of medical diagnosis by using motion information in image sequences. The studied algorithms could be applied in the case of the diagnosis of heart diseases, thyroid nodular diseases, arteriosclerosis and other diseases that imply the uses of image sequences. The paper aim to underline some advantages and disadvantages of several differential motion estimation methods in order to allow to ease choose a certain motion estimation method for a certain application. The studied methods will be tested on MRI (Magnetic Resonance Imaging) images but the methods are not limited only to this kind of data.***

Keywords: ***motion estimation, medical diagnosis, differential methods, optical flow.***

I. INTRODUCTION

The motion information is uses more and more in medical diagnosis. The analysis of temporal image sequences gives access to quantitative parameters of the organ's physiology and of their functioning [9]. This dynamic character is fundamental in medicine and particularly in the cardiovascular domain because the cardiovascular affections represent one of the principal causes of mortality in the industrialized countries [14]. To prevent or to diagnose these causes, there exist many methods based on the medical image processing and analysis. These images could be acquired by using different complementary methods as: X-rays (computer tomography CT, classical radiographies etc), ultrasounds (US imaging), magnetic resonance (MR imaging) or positron emission (PET positron emission tomography). There also are combined acquisition methods and data fusion methods, in order to obtain more complex information regarding the patient [15].

As it was mentioned above, the dynamic character is fundamental in the cardiovascular domain. For example, the motion estimation and analysis could offer information about arterial pulsatility and about the elasticity of the blood vessels. In the case of arteriosclerosis or a stenosis, the biomechanical properties of the arterial vessel are affected. This affection has a direct effect on local elasticity and thus on the hemodynamic behavior of the blood vessel. The worst consequence of a vascular stenosis is the infarcts. This affection determines the necrosis of cardiac cells that could determine, depending on its gravity, the infarct [3].

Until now, the using of image sequences to diagnose the cardiovascular diseases had a subjective character, the decision of the doctor depending on its experience in analyzing the images visualized on the screen of the acquisition tool. The objective information accessible to the doctor is obtained by measuring some electric parameters of the heart that are transformed into data concerning the cardiac cycle, useful for the doctors [10].

We are proposing in this paper to obtain some objective quantitative parameters extracted from image sequences that could be represented in an easy to use and interpret way for doctors. These parameters will be extracted by applying some motion estimation methods to medical image sequences. The most used methods could be divided in two great classes [8]:

- deterministic methods;
- stochastic methods.

In the class of stochastic methods, the most used are the Monte-Carlo type methods, Metropolis and Gibbs methods. These methods had the advantage that allow very precise results, but with a very high computational cost. The algorithms could have a computational time about hours, in the case of temporal three-dimensional image sequences. This is the reason why, in practice, it is preferred to use deterministic methods. These methods, even they not offer a high precision, they have a computational time that allow a real-time implementation [1].

Among the deterministic methods, the most used are the differential methods and the block-matching methods with their derivates [2]. The differential methods have the advantage of a small computational time, but they have the disadvantage that are limited to estimate only small displacements (2-3 pixels) because of the limited possibilities to numerically implement the finite differences in the computation of partial derivatives in this methods. The block matching methods have the advantage that are not limited to small displacements, but the computational time exponentially increases with the maximal displacement that should be estimated. In addition, these methods are not taking into account the motion discontinuity in the movement of the objects [12].

II. MOTION ESTIMATION METHODS

The images usually represent the projection of the real 3D scenes in the image plane. This is the reason why the observed motion (or the apparent motion) in a temporal image sequence represents the projection of the 3D motion in the image plane and it could be perceived as a changing of the spatial distribution of the intensity. The motion observed starting from the changing of the spatial distribution of the intensity represents the apparent motion or the optical flow and is usually different form the real motion [5].

The aim of the motion estimation methods is to estimate the motion field starting from a temporal image sequence with a content that varies during the time.

One of the hypotheses that have to be made in almost all the motion estimation methods, in order to can estimate the motion starting from the observed or apparent motion, is that the image intensity is constant during the movement or is changing in a predictable way [6]. This hypothesis of intensity preservation could be expressed through the so-called displaced frame difference (DFD) equation:

$$DFD(\boldsymbol{p}) = I_t(\boldsymbol{p}) - I_{t-1}(\boldsymbol{p} - \boldsymbol{d}(\boldsymbol{p})) \qquad (1)$$

where $\boldsymbol{p}=(x,y)$ is the position of a pixel of the image, I_t and I_{t-1} are the intensity images at t and t-1 instants and $\boldsymbol{d}(\boldsymbol{p})=(d_x(\boldsymbol{p}), d_y(\boldsymbol{p}))$ is the displacement of the pixel $\boldsymbol{p}$. Almost all the motion estimation methods are based on the minimization, one way or other, of the DFD equation.

The most used methods could be divided in two great classes [13], [16]:

- deterministic methods;
- stochastic methods.

The most used stochastic methods are the Monte-Carlo type methods, Metropolis and Gibbs methods. These methods had the advantage that allow very precise results, but with a very high computational cost. The algorithms could have a computational time about hours, in the case of temporal three-dimensional image sequences [6]. This is the reason why, in practice, it is preferred to use deterministic methods. These methods, even they not offer a high precision, they have a computational time that allow a real-time implementation [5].

The most used deterministic methods are the differential methods and the block-matching methods with their derivates [2], [5], [13]. The block matching methods have the advantage that they are not limited to small displacements, they are very intuitive and thus very ease to be hardware implemented but the computational time exponentially increases with the maximal displacement that should be estimated. The fact that these methods are not taking into accounts the motion discontinuity in the movement of the objects is another disadvantage of the block matching methods [2], [13].

III. DIFFERENTIAL MOTION ESTIMATION METHODS

The hypothesis of intensity preservation expressed by the DFD equation (1) could be rewritten as:

$$\frac{dI(x,y,t)}{dt} = 0 \qquad (2)$$

where x and y vary along the motion trajectory. Under the hyphotesis of spatio-temporal differentiability of the intensity and using the known differentiation rules [4], we obtain:

$$I\left(x+d_x, y+d_y, t+\Delta t\right) = I(x,y,t) + \frac{\partial I(x,y,t)}{\partial x} d_x + \frac{\partial I(x,y,t)}{\partial y} d_y + \frac{\partial I(x,y,t)}{\partial t} \Delta t + tos \qquad (3)$$

where tos denotes the terms of superior orders. Replacing this development in the DFD equation and neglecting the terms of superior orders, we obtain:

$$I\left(x+d_x, y+d_y, t+\Delta t\right) = I(x,y,t) + \frac{\partial I(x,y,t)}{\partial x} d_x + \frac{\partial I(x,y,t)}{\partial y} d_y + \frac{\partial I(x,y,t)}{\partial t} \Delta t + tos \qquad (3)$$

where tos denotes the terms of superior orders. Replacing this development in the DFD equation and neglecting the terms of superior orders, we obtain:

$$DFD(x,y,t) = 0 \qquad (4)$$

$$\frac{\partial I(x,y,t)}{\partial x} d_x + \frac{\partial I(x,y,t)}{\partial y} d_y + \frac{\partial I(x,y,t)}{\partial t} \Delta t = 0$$

Dividing by the time distance between images (time sampling distance) we obtain the so-called "optical flow equation" OFE [4], [11]: (5)

$$\frac{\partial I(x,y,t)}{\partial x} v_x(x,y,t) + \frac{\partial I(x,y,t)}{\partial y} v_y(x,y,t) + \frac{\partial I(x,y,t)}{\partial t} = 0$$

where $v_x(x,y,t)=d_x/\Delta t$, $v_y(x,y,t)=d_y/\Delta t$ are the two velocity compenents. This OFE could be rewritten as:

$$I^x \cdot v_x + I^y \cdot v_y + I^t = 0, \qquad \text{or:} \qquad (6)$$

$$\langle \nabla I, \boldsymbol{v} \rangle + \frac{dI}{dt} = 0 \qquad \text{where}$$

$$\nabla I = \left(\frac{\partial I}{\partial x}, \frac{\partial I}{\partial y} \right) = \left(I^x, I^y \right)$$

is the spatial gradient with the two components $I^x = \frac{\partial I}{\partial x}$ and $I^y = \frac{\partial I}{\partial y}$, $I^t = \frac{\partial I}{\partial t}$ is the temporal gradient and $\langle \cdot , \cdot \rangle$ represents the scalar product between two variables.

The differential methods have the advantage of a small computational time, but they have the disadvantage that are limited to estimate only small displacements (2-3 pixels) because of the limited possibilities to numerically implement the finite differences in the computation of partial derivatives in this methods.

As it can be noticed, the OFE is not sufficient to uniquely determine the motion field because the OFE represent only one equation with two unknowns (v_x and v_y) for each pixel. In order to completely determine the motion field it has to be introduced supplementary constraints.

In the case of the Horn and Schunck (HS) method [4], the additional constraint is the uniformity constraint that could be expressed by the following term that has to be minimized with the OFE: (7)

$$\xi^2_{uniformity} = \left(\frac{\partial v_x}{\partial x} \right)^2 + \left(\frac{\partial v_x}{\partial y} \right)^2 + \left(\frac{\partial v_y}{\partial x} \right)^2 + \left(\frac{\partial v_y}{\partial y} \right)^2$$

In the case of the Lucas and Kanade (LS) method [7], the same uniformity constraint (7) is applied to images but in a local manner. So, if in the case of the Horn and Schunck method a global uniformity of the motion field is imposed to the hole image, in the case of the Lucas and Kanade algorithm a local uniformity is imposed. This local application of the uniformity constraint allow to better preserve the motion discontinuities, even if not as it has to be preserved.

In the case of the mean-field annealing (MFA) method [17], a composed energy has to be minimised:

$$U(I,\boldsymbol{d},\boldsymbol{l}) = U_a(I,\boldsymbol{d}) + \alpha_d \cdot U_{dl}(\boldsymbol{d},\boldsymbol{l}) + \alpha_l \cdot U_l(\boldsymbol{l}) \qquad (8)$$

where: $U_a(I,\boldsymbol{d})$ is the energy attached to the data;

$U_{dl}(\boldsymbol{d},\boldsymbol{l})$ is the regularization energy for the displacement (or motion) field;

$U_l(\boldsymbol{l})$ is the regularization energy for the line field $\boldsymbol{l}$.

As an energy attached to the data in (8) it can be used the following forms for this term [18]: (9)

$$U_a(I,\boldsymbol{d}) = \frac{1}{2\pi\sigma_1^2} \sum_{\boldsymbol{p}} \left[I_t(\boldsymbol{p}) - I_{t-1}(\boldsymbol{p} - \boldsymbol{d}(\boldsymbol{p})) \right]^2 = \sum_{\boldsymbol{p}} \left[DFD(\boldsymbol{p}) \right]^2$$

or: (10)

$$U(I,\boldsymbol{d}) = \sum_{\boldsymbol{p}} \left\{ \frac{1}{2\pi\sigma_1^2} \left[d_x(\boldsymbol{p}) \cdot I^x(\boldsymbol{p}) + d_y(\boldsymbol{p}) \cdot I^y(\boldsymbol{p}) + I^t(\boldsymbol{p}) \right]^2 \right.$$

As regularization energy for the displacement (or motion) field in (8) it can be used the following forms for this term: (11)

$$U_{dl}(\boldsymbol{d},\boldsymbol{l}) = \frac{1}{2\pi\sigma_2^2} \cdot \sum_{\boldsymbol{r} \in N_{\boldsymbol{p}}} \left[\left\| \boldsymbol{d}(\boldsymbol{p}) - \boldsymbol{d}(\boldsymbol{r}) \right\|^2 \cdot (1 - \boldsymbol{l}(\boldsymbol{p},\boldsymbol{r})) \right]$$

where $\boldsymbol{r}$ are the pixels from the neighborhood $N_{\boldsymbol{p}}$ of the current pixel $\boldsymbol{p}$.

As regularization energy for the line field $\boldsymbol{l}$ in (8) it can be used the following forms for this term:

$$U_l(\boldsymbol{l}) = \sum_{\boldsymbol{p}} \left(\alpha_H \cdot H_{\boldsymbol{p}} + \alpha_V \cdot V_{\boldsymbol{p}} \right) \qquad (12)$$

where α_H and α_V are the corresponding weighting terms of the horizontal and vertical line field.

The line field $\boldsymbol{l}$ is introduced in order to take into account motion discontinuities. We can use an explicit binary "line process" that will mark the discontinuities, as in figure 1 [18].

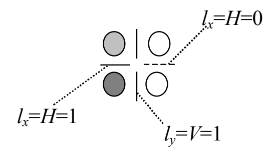

Figure 1. Illustration of the explicit binary line process.

Thus, an example of a composed energy that could be used in the case of the MFA method is [17]:

$$U(I,\boldsymbol{d},\boldsymbol{l}) = \sum_{i,j} \left\{ \frac{1}{2\pi\sigma_1^2} \left[I_t(i,j) - I_{t-1}((i,j) - \boldsymbol{d}_{i,j}) \right]^2 + \right.$$

$$+ \frac{\alpha_d}{2\pi\sigma_2^2} \cdot \left[\left\| \boldsymbol{d}_{i,j} - \boldsymbol{d}_{i,j-1} \right\|^2 \cdot (1 - H_{i,j}) + \left\| \boldsymbol{d}_{i,j} - \boldsymbol{d}_{i-1,j} \right\|^2 \cdot (1 - V_{i,j}) \right] +$$

$$\left. + \alpha_H \cdot H_{i,j} + \alpha_V \cdot V_{i,j} \right\} \qquad (13)$$

where $\boldsymbol{l}=(\boldsymbol{l}_x,\boldsymbol{l}_y)=(H,V)$ is the line process (or line field), with the two components: H (horizontal) and V (vertical), σ_1 and σ_2 are the standard deviations of the displacement field and line field, respectively, whereas α_d, α_H and α_V, are weighting coefficients of motion field and line field, respectively.

The simplest application of this algorithm implies the computation of the mean of each variable in a 4-neighborhood.

IV. EXPERIMENTAL RESULTS

In this Section, we present some comparative results, in terms of precision and computational time, between the Horn & Schunck (HS) method, the Lucas & Kanade (LS) method and the MFA algorithm.

In figure 2, the experimental results on a real MRI sequence (of 25 images) are presented. This sequence is obtained using a MRI imaging method of a human heart.

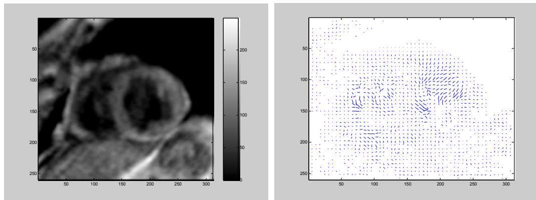

(a) (b)

Figure 2. Results in the case of IRM sequence.

In figure 2 (a) the first image of the real sequence (MRI) is presented. In figure 2 (b) the estimated motion field is illustrated. The motion field was estimated using the MFA algorithm.

In table 1, the comparative numerical results are presented, for HS, LS and MFA method, in the case of the MRI sequence.

TABLE 1. COMPARATIVE RESULTS FOR MRI SEQUENCE.

Estimation method	Mean Value	Standard Deviation
HS	-0.14	1.17
LS	0.11	1.14
MFA	-0.103	1.02

As we can observe from the above results, the most accurate results are obtained with the MFA estimation method.

In terms of computational time, the MFA method's results are comparable to those given by the HS algorithm.

TABLE 2. COMPARATIVE COMPUTATIONAL TIME.

	HS	LS	MFA
Computational time [s]	0.5	0.7	0.8

The computational time could be further reduced for all these algorithms by using multi-resolution techniques.

V. CONCLUSIONS

In this paper we presented a comparative study between three differential motion estimation methods that could be applied in the case of medical diagnosis by using motion information in image sequences. The studied algorithms could be applied in the case of the diagnosis of heart diseases, thyroid nodular diseases, arteriosclerosis and other diseases that imply the uses of image sequences. The paper underlined some advantages and disadvantages of the three motion estimation methods in order to allow to ease choose a certain motion estimation method for a certain application. The studied methods were tested on MRI (Magnetic Resonance Imaging) images but the methods are not limited only to this kind of data.

REFERENCES

[1] Barron J.L., Fleet D.J., Beauchemin S.S., ”Performance of optical flow techniques”, International Journal of Computer Vision, Vol.12, No.1, pp. 43-77, 1994.

[2] Giachetti A., „Matching techniques to compute image motion”, Image vision and computing, pp. 247-260, 2000.

[3] Hemmendor M., “Motion Estimation and Compensation in Medical Imaging – A survey”, Department of Biomedical Engineering, LinkAoping, Sweden, 168 pages, 2001.

[4] Horn B.K.P., Schunck B.G., “Determining Optical Flow”, Artificial Intelligence, Vol.17, p. 185-203, 1981.

[5] Konrad J., ”Motion detection and estimation”, Image Processing Handbook, Networking and Multimedia, pp. 207-227, 2000.

[6] Liu H., Herman M., Camus T., Chellappa R., ”Accuracy vs Efficiency trade-offs in optical flow algorithms”, Computer Vision and Image Understanding, Vol.72, No.3, pp. 271-286, 1998.

[7] Lucas B.D., Kanade T., „An Iterative Image Registration Technique”, Proceedings of Imaging Understanding Workshop, pp. 121-130, 1981.

[8] Nagel H.-H., ”On the estimation of optical flow: Relations between different approaches and some new results”, Artificial Intelligence, Vol.33, pp. 299-324, 1987.

[9] Ophir J., Céspedes I., Ponnekanti H., Yazdi Y., Li X., “Elastography: a quantitative method for imaging the elasticity of biological tissues”, Ultrasonic Imaging, 13(2), pp. 111-134, 1991.

[10] Revell J., Mirmehdi M., McNally D., “Computer vision elastography: speckle adaptive motion estimation for elastography using ultrasound sequences”, IEEE Transactions on Medical Imaging, 24(6), pp. 755-766, 2005.

[11] Shi B. E., Roska T., Chua L. O., ”Estimating optical flow with cellular neural networks”, International Journal of Circuit Theory and Applications, Vol.26, pp. 343-364, 1998.

[12] Stiller C., Konrad J., ”Estimating motion in image sequences – A tutorial on modeling and computation of 2D motion”, IEEE Signal Processing Magazine, pp. 70-91, 1999.

[13] Stiller C., Konrad J., ”On models, criteria and search strategies for motion estimation in image sequences”, IEEE Signal Processing Magazine, pp. 1-41, 1998.

[14] Suhling M., Arigovindan M., Hunziker P., Unser M., “Myocardial motion analysis from B-mode echocardiograms”, IEEE Transactions on Image Processing, 14(4), pp. 525-536, 2005.

[15] Webb S., “The physics of medical imaging”, Institute of Physics Publishing, London, Medical Science Series, 1998.

[16] Wechsler H., Duric Z., Li F., Cherkassky V., “Motion estimation using statistical learning theory”, IEEE Transactions on Pattern Analysis and Machine Intelligence, 26(4), pp. 466-478, 2004.

[17] Yu Tian T., Shah M., ”Motion segmentation and estimation”, Machine and Vision Applications, Springer-Verlag, Vol.9, pp. 32-42, 1996.

[18] Zhang J., Hanauer G., ”The application of mean field theory to image motion estimation”, IEEE Trans. on Image Processing, Vol.4, No.1, pp. 19-33, 1995.